PCCP

PAPER

View Article Online
View Journal | View Issue



Cite this: *Phys. Chem. Chem. Phys.*, 2017, **19**, 12970

# Antiradical activity of catecholamines and metabolites of dopamine: theoretical and experimental study†

D. Dimić, [a] D. Milenković, [b] J. Dimitrić Marković [a] and Z. Marković *[c]

The importance of molecules with antiradical potency that are produced in the human body has significantly increased. Among others, neurotransmitters and their metabolites act as the first line of defense against oxidative stress in the peripheral endocrine and the central nervous systems. Dopamine (DO), epinephrine (EP), norepinephrine (NE), L-DOPA, catechol, and three metabolites of dopamine (3-methoxytyramine (3-MT), homovanillic acid (HO), and 3,4-dihydrophenylacetic acid (DOPAC)) were investigated for their antiradical potency *via* computational methods and DPPH assay. Density functional theory calculations were used to determine the most probable reaction mechanism based on the thermodynamic parameters. These results suggested that hydrogen atom transfer (HAT)/proton-coupled electron transfer (PCET) and sequential proton loss electron transfer (SPLET) mechanisms are preferable in polar solvents. Several techniques were employed to differentiate between HAT and PCET mechanisms *via* examination of the transition state structures. Kinetic studies of HAT/PCET and electron transfer (ET) reactions, the second step of SPLET, have proven that ET is much faster for an order of $10^5$–$10^6$. Based on this, it was concluded that SPLET was the dominant mechanism for the antiradical activity towards DPPH radicals in polar solvents. The findings suggest that all the investigated molecules can be classified as excellent antiradical scavengers, except for 3-MT and homovanillic acid.

Received 17th March 2017,
Accepted 24th April 2017

DOI: 10.1039/c7cp01716b

rsc.li/pccp



## Introduction

Free radicals, chemical species with unpaired electron(s), are usually produced by a normal aerobic metabolism and also by other processes and agents such as smoking, herbicides and pesticides, drugs, ionizing radiation, and pollutants. Although they are necessary to life, excess amounts can shift the balance between oxidant and antioxidant statuses, causing oxidative stress.[1–3] When oxidative stress occurs, organisms attempt to restore the redox balance by activation of internal and external antioxidants. Oxidative stress is assumed to play an important role in the pathogenesis of many, if not all, diseases such as hypertension, inflammation, cancer, cardiovascular disease, and neurodegenerative disorders such as Parkinson's, Alzheimer's, and Huntington's disease.[3]

Generally, all neurodegenerative disorders are characterized by changes in nerve cells at the molecular level that result in cell degeneration and death. Besides the changes in neurotransmitter concentrations, oxidative stress, which causes lipid peroxidation and protein structural changes, is essentially found to be the origin of these diseases.[4–9]

Dopamine, norepinephrine, and epinephrine are catecholamines that function as hormones and neurotransmitters in the peripheral endocrine and the central nervous systems.[10–13] They are involved in movement control and posture, mood modulation, decision-making, reward processing, attention, working memory and learning, attentiveness, emotions, sleeping, and dreaming. The above-mentioned molecules are produced from tyrosine through a step that includes 3,4-dihydroxy-L-phenylalanine (L-DOPA).[14] In this complex mechanism, dopamine is decomposed to several molecules, including 3,4-dihydroxyphenylacetic acid, homovanillic acid, and 3-methoxytyramine. The most important metabolite of dopamine in the brain is 3,4-dihydroxyphenylacetic acid (DOPAC).[15,16] It is produced by a two-step oxidation mechanism catalyzed by aldehyde dehydrogenase and monoamine oxidase. Homovanillic acid (4-hydroxy-3-methoxyphenylacetic acid) differs from DOPAC by one methoxy group, and its role as a neurotransmitter is also known.[17] The extracellular metabolite of dopamine, 3-methoxytyramine (3-MT),

[a] *Faculty of Physical Chemistry, University of Belgrade, 12-16 Studentski trg, 11000 Belgrade, Republic of Serbia*
[b] *Bioengineering Research and Development Center, Prvoslava Stojanovića 6, 34000 Kragujevac, Republic of Serbia*
[c] *Department of Chemical-Technological Sciences, State University of Novi Pazar, Vuka Karadžića bb, 36300 Novi Pazar, Republic of Serbia. E-mail: zmarkovic@np.ac.rs*

† Electronic supplementary information (ESI) available. See DOI: 10.1039/c7cp01716b

is produced by catechol-*O*-methyltransferase and it represents a neuromodulator;[18] elevated concentrations of this can be indicative of brain and carcinoid tumors,[19] schizophrenia, and Parkinson's disease.[20,21] All the above-mentioned molecules, except for 3-MT and homovanillic acid, contain the catechol moiety, and this is the reason why catechol is simultaneously investigated.

Because these molecules play such diverse roles in human behavior and cognition and have extraordinarily important functions *in vivo*, they continue to receive considerable research attention.[11–13,22] The facts that suggest an association between neurodegenerative diseases and oxidative stress indicate that antioxidants can potentially act as therapeutic agents.[22] More than 20% of the body's oxygen is used in the brain, so the above-mentioned neurotransmitters are exposed to significant amounts of reactive oxygen species.[23,24] Also, in this tissue there is a considerable amount of unsaturated fatty acids that are highly susceptible to oxidation. The limited permeation through the blood–brain barrier (BBB) of the external antioxidants leads to increased attention to molecules synthesized in the brain itself.[25]

Several *in vitro* experimental studies have been conducted on the antiradical activity of catecholamines and some of their structural analogues or metabolites, proving their significant reactivity towards biologically relevant radicals.[14,26–30] Detailed quantum-chemical calculations of the reactivity of dopamine,[31] norepinephrine, and epinephrine[32] towards hydroxyl and hydroperoxyl radicals have been performed, and a multitude of possible reaction pathways with different probabilities have been found. It was also concluded that, under the proper conditions, all the above-mentioned molecules can be regenerated to their original form.[32]

For the above reasons, there is a constant need to understand the role of the investigated molecules in the overall antiradical activity. Moreover, this type of activity is very common for molecules containing the catechol moiety.

Different reaction mechanisms between antiradical molecules and radicals have been proposed. They can generally be grouped into two types of processes: H-atom abstraction and radical adduct formation. H-atom abstraction processes may occur *via* at least four different mechanisms: hydrogen atom transfer (HAT), proton coupled electron transfer (PCET), sequential proton loss electron transfer (SPLET), and single electron transfer followed by proton transfer (SET-PT).[33,34] All the mechanisms have the same net results.

The HAT mechanism is characterized by rapid hydrogen atom transfer from a molecule (ArOH) to a free radical:

$$\mathrm{ArOH} + \mathrm{R}^{\bullet} \rightarrow \mathrm{ArO}^{\bullet} + \mathrm{RH} \quad (1)$$

The PCET mechanism gives the same products as the HAT mechanism, but electrons and protons are transferred in a single kinetic step *via* different routes. The PCET mechanism is present in many biological and biochemical processes with significant implications.[35,36] These two mechanisms will be considered together (noted as HAT/PCET) in the first part of this paper, but for the transition state structures for reactions with DPPH, these two are differentiated and explained in detail.

The SPLET mechanism is a two-step mechanism that includes the successive formation of an anion and a radical of the investigated molecule (eqn (2a) and (2b)) and protonation of the radical anion (eqn (2c)).

$$\mathrm{ArOH} \rightarrow \mathrm{ArO}^{-} + \mathrm{H}^{+} \quad (2a)$$

$$\mathrm{ArO}^{-} + \mathrm{R}^{\bullet} \rightarrow \mathrm{ArO}^{\bullet} + \mathrm{R}^{-} \quad (2b)$$

$$\mathrm{R}^{-} + \mathrm{H}^{+} \rightarrow \mathrm{RH} \quad (2c)$$

The SET-PT mechanism implies two steps, the first in which the molecule loses an electron, yielding the corresponding radical cation (eqn (3a)), and the second in which the radical cation is deprotonated (eqn (3b)).

$$\mathrm{ArOH} + \mathrm{R}^{\bullet} \rightarrow \mathrm{ArOH}^{\bullet+} + \mathrm{R}^{-} \quad (3a)$$

$$\mathrm{ArOH}^{\bullet+} + \mathrm{R}^{-} \rightarrow \mathrm{ArO}^{\bullet} + \mathrm{RH} \quad (3b)$$

The present paper comprises *in vitro* experimental and theoretical approaches proposing a possible explanation for the antiradical activity of major catecholamines (dopamine, norepinephrine, and epinephrine), catechol, L-DOPA, and three metabolites of dopamine (3-methoxytyramine, homovanillic acid, and 3,4-dihydroxyphenylacetic acid). As a model system, the DPPH radical and its corresponding assay are used. The thermodynamic and mechanistic schemes were employed for the theoretical description of reactions.

## Experimental

The investigated compounds, dopamine hydrochloride, 3-methoxytyramine hydrochloride (3-MT), epinephrine, norepinephrine hydrochloride, catechol, homovanillic acid, L-3,4-dihydroxyphenylalanine (L-DOPA), 3,4-dihydroxyphenyl acetic acid (DOPAC), and 2,2-diphenyl-1-picrylhydrazyl (DPPH), were purchased from Aldrich Chemical Co. The chemicals were of reagent grade.

The DPPH radical scavenging activity was measured using a method described in a previous contribution.[37] The concentration of DPPH was held constant (0.1 mM) and the concentrations of the selected molecules varied from 0.01 to 0.4 mM. A Cintra GB-10 UV-Vis spectrometer was used to monitor the change in concentration of DPPH at 517 nm. $EC_{50}$ values were obtained for all the investigated molecules and are presented in Table 1.

## Computational methods

All the calculations were performed using the Gaussian Program Package.[38] The equilibrium geometries of neurotransmitters and metabolites, as well as their radicals, radical cations, and anions, were optimized with the empirical exchange–correlation functional M06-2X[39] and the split valence basis set 6-311++G(d,p).[40] This combination of basis set and functional was used in numerous studies for the calculation of antiradical parameters.[41–43]

The absence of imaginary frequencies proved that the local and global minima were found. In order to account for the solvent effects, three solvents were investigated (water, methanol,

Table 1 Antiradical activity, HOMO and LUMO energies, energy gaps, and stabilization energies of the investigated molecules

| Compound | $EC_{50} \times 10^{-6}$ | Stoichiometric factor | HOMO (eV) | LUMO (eV) | HOMO–LUMO gap | $\Delta E_{iso}$ (kJ mol$^{-1}$) |
|---|---|---|---|---|---|---|
| Catechol | 13.92 ± 0.05[a]<br>11.9[c] | 4.20 | −0.295 | 0.053 | 0.348 | −31.32 |
| Homovanillic acid | 26.6[c] | 1.88 | −0.296 | 0.044 | 0.341 | −24.32 |
| 3-MT | 63.16 ± 0.91[a]<br>36.1[c] | 1.38 | −0.291 | 0.057 | 0.348 | −29.32 |
| Dopamine | 10.50 ± 0.51[a]<br>10.5[c] | 4.76 | −0.290 | 0.056 | 0.346 | −37.32 |
| DOPAC | 7.1[b]<br>7.8[c] | 6.41 | −0.295 | 0.044 | 0.340 | −33.32 |
| Epinephrine | 11.27 ± 0.01[a]<br>10.5[c] | 4.76 | −0.294 | 0.055 | 0.349 | −36.32 |
| Norepinephrine | 10.87 ± 0.12[a]<br>10.6[c] | 4.72 | −0.294 | 0.055 | 0.350 | −35.32 |
| L-DOPA | 5.67 ± 0.01[a]<br>6.9[c] | 7.24 | −0.293 | 0.036 | 0.328 | −63.32 |

[a] Ref. 26. [b] (In ethanol) ref. 57. [c] Measurements from this study.

and benzene) using the implemented SMD method.[44] The solvent effects were taken into account for all the investigated species. The selected solvents were used in order to obtain valuable data about the change in thermodynamic parameters in polar (water and methanol) and non-polar (benzene) environments. The antiradical DPPH assay used was performed in methanol, and this was an additional reason for the optimizations in this solvent. NBO analysis[45] of all species was obtained at the mentioned level of theory. This approach was used to obtain a better insight into the stabilizing and destabilizing interactions between the occupied and unoccupied orbitals.

The thermodynamic parameters governing the mentioned mechanisms are: the Bond Dissociation Energy (BDE) of ArOH in the HAT/PCET mechanism, the Ionization Potential (IP) of ArOH and the Proton Dissociation Enthalpy (PDE) of $ArOH^{+\bullet}$ in the SET-PT mechanism, the Proton Affinity (PA) of ArOH, and the Electron Transfer Enthalpy (ETE) of $ArO^-$ in the SPLET mechanism. These values were calculated from the enthalpies of the respective species as shown by eqn (4)–(8).[46,47]

$$BDE = H(ArO^{\bullet}) + H(H^{\bullet}) - H(ArOH) \quad (4)$$

$$IP = H(ArOH^{\bullet+}) + H(e^-) - H(ArOH) \quad (5)$$

$$PDE = H(ArO^{\bullet}) + H(H^+) - H(ArOH^{\bullet+}) \quad (6)$$

$$PA = H(ArO^-) + H(H^+) - H(ArOH) \quad (7)$$

$$ETE = H(ArO^{\bullet}) + H(e^-) - H(ArO^-) \quad (8)$$

The thermodynamic parameters were calculated at 298 K for species optimized by employing the SMD method with methanol as solvent. The enthalpies for protons and electrons were taken from the literature.[48] One of the important parameters, the radical stability, was determined as the stabilization energy ($\Delta E_{iso}$) by taking the reaction with phenol (PhOH) and the phenoxy radical ($PhO^{\bullet}$) into account:

$$\Delta E_{iso} = H(ArO^{\bullet}) + H(PhOH) - H(ArOH) - H(PhO^{\bullet}) \quad (9)$$

The transition state structures (TS) were obtained by synchronous transit guided quasi-Newton methods at the M06-2X/6-31G(d,p) level of theory. The intrinsic reaction coordinates (IRC), as implemented in the Gaussian program package, were traced to the reactant complex (RC) and product complex (PC), both of which are considered as single structures. The RC and PC, taken from the IRC routine, were additionally optimized without movement restrictions. The optimization and energy calculation for the TS, RC, and PC did not include any constraints to separate charges; therefore, the global charge and spin multiplicity were the same for all the mentioned structures. The obtained structures were verified by normal mode analysis to be minima (no imaginary frequencies, PC and RC) or maxima (one imaginary frequency, TS) on the potential energy surface.

Rate constants were calculated using TheRate program[49] for a 1 M standard state. Based on conventional transition state theory (TST), the rate constant is calculated as follows:

$$k_{HAT/PCET} = \sigma\kappa\frac{k_B T}{h}\exp\left(-\frac{\Delta G^{\ddagger}}{RT}\right) \quad (10)$$

In the previous equation, $k_B$ and $h$ are the Boltzmann and Planck's constants, $\Delta G^{\ddagger}$ is the free activation energy, $\sigma$ is the reaction path degeneracy, which counts the possible reaction pathways, and $k$ is the tunneling correction. The thermodynamic data and partition functions were taken from the quantum chemical calculations. The tunneling correction was calculated as the Boltzmann average of the ratio between the quantum and classical probabilities and was calculated using the zero-tunneling approach.

Together with the HAT/PCET investigation, the Marcus theory[50] was applied in order to kinetically examine the electron transfer (ET) mechanism. The activation barrier for this reaction depends on two thermodynamic parameters – the free energy of the reaction and the nuclear reorganisation energy as follows:

$$\Delta G_{ET}^{\ddagger} = \frac{\lambda}{4}\left(1 + \frac{\Delta G_{ET}^{0}}{\lambda}\right)^2 \quad (11)$$

In the previous equation, $\lambda$ is the reorganizational energy, which is defined as the difference between the nonadiabatic energy difference between reactants and products and the activation barrier:

$$\lambda \approx \Delta E_{ET} - \Delta G_{ET}^{0} \quad (12)$$

 

Theoretical investigation of the various reactions showed that the calculated rate constant can be comparable to the diffusion-limited rate constant. Therefore, the apparent rate constant ($k_{app}$) is calculated according to the Collins–Kimball theory.[51] In order to obtain this value, the steady-state Smoluchowski rate constant ($k_D$)[31] has to be calculated under the assumption of the irreversible bimolecular diffusion-controlled reaction. Both the formulas are shown:

$$k_{app} = \frac{k_D k}{k_D + k} \quad (13)$$

$$k_D = 4\pi R D_{AB} N_A \quad (14)$$

The parameters have the following meaning: $R$ is the reaction distance, $D_{AB}$ is the diffusion coefficient of the reactants, in this case the DPPH radical and antioxidants, and $N_A$ is Avogadro's constant. The parameter $D_{AB}$ can be calculated from $D_A$ and $D_B$, which on the other hand are estimated from the Stokes–Einstein approach:

$$D = \frac{k_B T}{6\pi\eta a} \quad (15)$$

The newly introduced parameters in this equation are the viscosity of the solvent, $\eta$, and $a$, which is the radius of the solvent.[31]

# Results and discussion

### DPPH antiradical scavenging activity

The DPPH antiradical activity (Table 1) of all the selected compounds (Fig. 1) was examined and this was proven to be in good accordance with the literature data.[26] The stoichiometric factor, calculated as $n = \frac{[DPPH]_0}{2EC_{50}}$, is usually taken as a complementary factor to the $EC_{50}$ value and for good antioxidants has a value of $n \geq 2$.[52] Although this parameter can be ambiguous because it depends on the concentration of DPPH and the measurement time, the experiments in this contribution were done with the same standard solution and for the same time. Based on these measurements, all the molecules have significant antiradical activity.

From Table 1, it can be concluded that all the molecules containing the catechol moiety have this parameter in the range of good antioxidants. The antiradical activity of L-DOPA and DOPAC is very similar to that of quercetin and gallic acid,[26] while dopamine, epinephrine, norepinephrine, and catechol have higher activity than the reference antioxidants – Trolox, ascorbic acid, and (+)-α-tocopherol.[26] For 3-MT and homovanillic acid, the values are slightly lower but still in the range of good antiradicals, as measured in the comprehensive study by Sârbu and coworker.[26]

From a structural point of view, the number of OH groups plays an important role in the antioxidant activity.[46] In this study, molecules with two OH groups attached to the aromatic ring have significantly lower $EC_{50}$ values and stoichiometric parameters than in the case when only one hydroxyl group is present. When the catechol moiety is present, high antiradical activity can be expected because of the ease of proton donation from these groups and the additional stabilization of the radicals formed, which is due to the formation of intramolecular hydrogen bonds. The computational methods were used for the in-depth analysis of the structural and electronic parameters governing the antioxidant activity, as described in the next few sections.

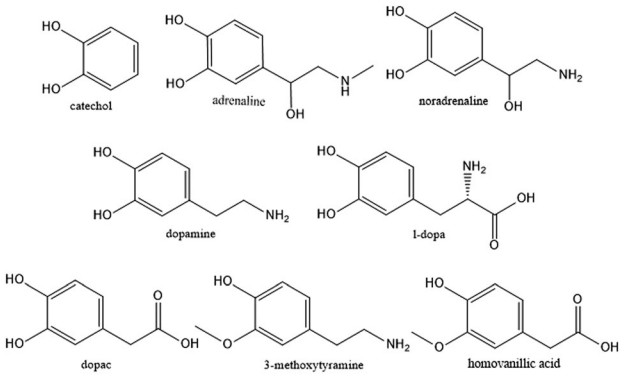


Fig. 1 Structures of investigated molecules.

### Thermodynamic parameters

Five of the most stable conformers for each of the molecules were taken from the literature and optimized again at the M06-2X/6-311++G(d,p) level of theory in three solvents water, benzene, and methanol.[15,17,53–56] All the substances were investigated in their neutral form because the experiments were performed in methanol, and significant protonation is not expected. The protonated forms of dopamine, epinephrine, norepinephrine, and 3-methoxytyramine might show different activity compared to neutral molecules, but this effect is not investigated in this contribution. The same applies to the anionic forms of the molecules. The most stable conformations of catecholamines and metabolites of dopamine in methanol are given in Fig. S1 (ESI†). The possible positions of XH (X = O, N) bond breakage and thermodynamic parameters, for all the investigated molecules, were determined and calculated. The structures of the corresponding radicals, radical cations, and anions were optimized from the structure of the most stable conformer.

From the structures shown in Fig. 1, it is possible to conclude that there are different numbers of ''active'' positions relevant to the antiradical activity of the selected molecules: one for catechol (because of the symmetry of the molecule), two for homovanillic acid (*p*-OH and COOH groups) and 3-MT (*p*-OH and $NH_2$ groups), and three for dopamine (two catechol OH and $NH_2$ groups), DOPAC (two catechol OH and COOH groups), epinephrine (two catechol OH and NH groups), norepinephrine (two catechol OH and $NH_2$ group), and L-DOPA (two catechol OH and COOH groups). Table 2 lists the thermodynamic parameters relevant to the antiradical activity mechanisms calculated according to eqn (4)–(8).

Table 2 Thermodynamic parameters for the three most common antiradical mechanisms for catecholamines and their metabolites (in kJ mol$^{-1}$)

| | | Aqueous phase | | | | | Benzene phase | | | | | Methanol phase | | | | |
|---|---|---|---|---|---|---|---|---|---|---|---|---|---|---|---|---|
| | | HAT/PCET | SET-PT | | SPLET | | HAT/PCET | SET-PT | | SPLET | | HAT/PCET | SET-PT | | SPLET | |
| Molecule | Site | BDE | IP | PDE | PA | ETE | BDE | IP | PDE | PA | ETE | BDE | IP | PDE | PA | ETE |
| Catechol | | | 490 | | | | | 656 | | | | | 508 | | | |
| | OH | 348 | | 21 | 139 | 372 | 334 | | 91 | 425 | 322 | 344 | | 11 | 137 | 382 |
| Homovanillic acid | | | 482 | | | | | 634 | | | | | 500 | | | |
| | *p*-OH | 354 | | 35 | 154 | 363 | 360 | | 139 | 469 | 304 | 351 | | 26 | 153 | 372 |
| | COOH | 412 | | 94 | 109 | 466 | 350 | | 129 | 426 | 337 | 413 | | 88 | 108 | 479 |
| 3-MT | | | 474 | | | | | 621 | | | | | 492 | | | |
| | *p*-OH | 349 | | 38 | 157 | 355 | 356 | | 148 | 478 | 291 | 346 | | 28 | 156 | 364 |
| | $NH_2$ | 412 | | 100 | 320 | 255 | 418 | | 210 | 644 | 187 | 414 | | 97 | 324 | 265 |
| Dopamine | | | 479 | | | | | 632 | | | | | 496 | | | |
| | *p*-OH | 342 | | 26 | 143 | 363 | 332 | | 113 | 424 | 321 | 338 | | 16 | 141 | 372 |
| | *m*-OH | 347 | | 31 | 141 | 369 | 328 | | 109 | 426 | 315 | 342 | | 21 | 139 | 378 |
| | $NH_2$ | 412 | | 96 | 320 | 255 | 418 | | 200 | 638 | 193 | 415 | | 93 | 323 | 266 |
| DOPAC | | | 487 | | | | | 649 | | | | | 504 | | | |
| | *p*-OH | 346 | | 22 | 140 | 369 | 335 | | 98 | 418 | 329 | 342 | | 21 | 137 | 379 |
| | *m*-OH | 347 | | 23 | 139 | 371 | 333 | | 96 | 419 | 327 | 343 | | 13 | 137 | 381 |
| | COOH | 418 | | 94 | 110 | 471 | 347 | | 111 | 422 | 338 | 418 | | 88 | 109 | 483 |
| Epinephrine | | | 483 | | | | | 631 | | | | | 498 | | | |
| | *p*-OH | 344 | | 24 | 140 | 367 | 330 | | 111 | 431 | 312 | 339 | | 15 | 136 | 377 |
| | *m*-OH | 346 | | 27 | 138 | 371 | 334 | | 116 | 432 | 315 | 341 | | 17 | 136 | 380 |
| | $NH_2$ | 384 | | 64 | 313 | 234 | 393 | | 174 | 577 | 229 | 388 | | 64 | — | — |
| Norepinephrine | | | 483 | | | | | 637 | | | | | 499 | | | |
| | *p*-OH | 345 | | 25 | 140 | 368 | 329 | | 105 | 439 | 303 | 340 | | 16 | 138 | 377 |
| | *m*-OH | 349 | | 28 | 140 | 372 | 332 | | 108 | 426 | 320 | 344 | | 20 | 138 | 381 |
| | NH | 422 | | 101 | 206 | 379 | 423 | | 199 | 577 | 259 | 425 | | 101 | 297 | 303 |
| L-DOPA | | | 471 | | | | | 659 | | | | | 474 | | | |
| | *p*-OH | 332 | | 24 | 131 | 364 | 331 | | 85 | 411 | 333 | 340 | | 13 | 139 | 375 |
| | *m*-OH | 335 | | 27 | 130 | 368 | 334 | | 87 | 408 | 339 | 342 | | 16 | 137 | 380 |
| | COOH | 417 | | 109 | 106 | 474 | 482 | | 235 | 429 | 466 | 429 | | 103 | 116 | 488 |

## HOMO and LUMO orbital energies

HOMO and LUMO energy differences can be useful parameters where the chemical reactivity is concerned. Higher energy of the HOMO orbital implies that a molecule is a better electron donor. Therefore, HOMO orbitals are visualized for all the investigated molecules in the ESI† (Fig. S2).

From the data presented in Table 1, it is evident that all the molecules have similar HOMO orbital energy values, although it is evident that molecules containing a carboxyl group have higher states, implying the importance of this group in the antiradical activity. L-DOPA had the lowest HOMO–LUMO energy gap, which indicates its high reactivity towards the radical species. As previously discussed, the presence of two OH groups and a carboxyl group gives a good basis for reactivity. The gap is generally low for molecules containing the carboxyl group because of the proximity of n and $\pi^*$ orbitals. It is interesting to notice that 3-MT has an energy gap similar to dopamine, proving that electrons of the methoxy group are not included in the formation of orbitals, while the corresponding $EC_{50}$ values are significantly different. The molecules of dopamine, epinephrine, and norepinephrine have almost the same energy gap, as reflected in the experimental antiradical activity. But it should be borne in mind that with a group of molecules that have distinct structural features, this type of analysis can be ambiguous.

## Stabilization energies

The stabilization energy method (eqn (9)) can be used to predict the possible antiradical activity towards different radicals.[58] The stabilization energy values in methanol shown in Table 1 successfully reflect the obtained experimental results. All the values are negative, predicting the possible antiradical activity and stability of the radicals formed from parent molecules. The importance of the additional hydroxyl group is proved by a change in the stabilization energy by several kJ mol$^{-1}$. Molecules containing the carboxyl group also have lower values. Again, L-DOPA was proven to have the highest antiradical activity.

## Bond dissociation enthalpy and proton affinity

The formation of radicals is possible when the OH or NH bonds are homolytically broken. The stability of the formed radicals plays an important role in the overall mechanism of the antiradical activity. There is no significant difference between

 

HAT/PCET values for polar solvents (water and methanol) and for benzene (Table 2). The geometries of molecules were equivalent in methanol and water for all the investigated molecules, and this explains small differences in the thermodynamic parameters in these two solvents. As can be observed in Table 2, the most stable radicals are formed when the OH bonds of the ring-bound groups are broken. The values of the BDE (Table 2) are influenced by the presence of the second OH group. The absence of the second OH group results in higher BDE values for 3-MT and homovanillic acid by up to 20 kJ mol$^{-1}$ in all solvents. For molecules with the catechol moiety, the BDE values for the two OH groups are very similar. One of the reasons for this might be the optimization of the radical structure that included groups positioned in the way that the intramolecular hydrogen bond is formed because this additionally stabilizes the structure. Immediately after deprotonation, before the second OH group rotation, the values of the BDE should be different and a lower value is expected for the *p*-OH group. The values of the BDE are very similar for the rest of the investigated molecules, proving that the presence of the aliphatic side chains does not significantly influence the bond breakage. This also proves that OH groups are more likely to be broken when compared to $NH_2$ groups, which on average need more energy, up to 40–80 kJ mol$^{-1}$. The BDE values for the carboxyl group are significantly higher than for the OH group, on average 70 kJ mol$^{-1}$, and according to the HAT mechanism, they are less likely to break when compared to the latter. The stability of radicals can be understood based on the delocalization of spin density and delocalization of the SOMO orbital (Fig. 2 and Fig. S2, ESI†). Radicals with good spin delocalization are easily formed and are more stable. In all the molecules, the unpaired electron is spread over the aromatic ring, with significant contribution on the oxygen atom in the *o*-position with respect to the broken OH bond. This proves that the aromatic ring and attached OH groups are the most important structural parameters with respect to the antioxidant activity. The SOMO orbitals of the investigated molecules show delocalization over the involved oxygen, the neighboring carbon atoms of the aromatic ring, and the second oxygen atom. Additional stabilization is due to delocalization inside the aliphatic group.

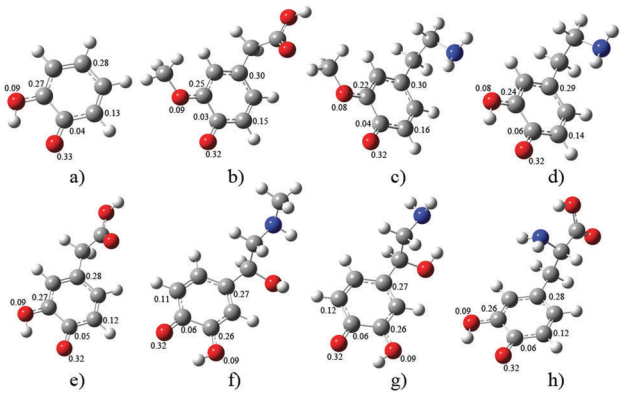


Fig. 2 Spin density distribution in the most stable radicals in methanol: (a) catechol, (b) homovanillic acid, (c) 3-MT, (d) dopamine, (e) DOPAC, (f) epinephrine, (g) norepinephrine, (h) L-DOPA.

The analysis of the SOMO orbital additionally confirms the high stability of the formed radicals.

In order to obtain more quantitative parameters for the stabilization of the respective radicals, NBO analysis has been performed. Based on the second order perturbation theory, there is an important donor–acceptor interaction between oxygen atoms in the formed radical and the *m*-OH group with respect to the aliphatic chain. The stabilization energy is 1.05 kJ mol$^{-1}$ (Table S3, ESI†). Table S3 (ESI†) also shows that the charge on the oxygen atom in the formed radical is similar for all the investigated molecules.

The heterolytic cleavage of OH and NH bonds leads to the formation of the corresponding anions, which is quantified by the values of the proton affinity listed in Table 2. These values show even higher resemblance in water and methanol. The values for the PA of the catechol moiety are approximately 140 kJ mol$^{-1}$ and they increase to 155 kJ mol$^{-1}$ when only one OH group is present, because no stabilization effect is present due to the formation of the hydrogen bond. The same effect of similar thermodynamic PA parameters for the two OH groups in the catechol moiety is observed and an equivalent explanation can be given. Lower values for the PA are found in the carboxyl groups, due to the stabilization effect of the charge delocalization inside –COO$^-$. It should be borne in mind that deprotonation of carboxyl groups is preferable in methanol and water and therefore these groups are not further investigated with respect to their antiradical activity, although their contribution is expected. This activity is probably very dependent on the pH of the solution. The PA values for amino groups are more than two times larger, probably due to the low stability of the –NH$^-$ group formed. The high values of the PA indicated that amino groups are probably not included in the mechanism of the antiradical activity. There is also a significant difference between the PA values of polar solvents and benzene, showing that this first step of the SPLET mechanism is thermodynamically more probable than HAT/PCET and is more likely to occur in polar solvents due to dipole–dipole interactions. In non-polar solvents, the order is reversed. The same stabilization effects of hydrogen bond formation can be seen in anions, with the stabilization energy being double that in radicals. Table S3 (ESI†) gives the charges on the oxygen atom of the broken OH bond. The negative charge is solely concentrated on this atom without further delocalization over the aromatic ring. Because of this, a stronger hydrogen bond than for the respective radicals is formed. The energy of this bond is about 2.2 kJ mol$^{-1}$ (Table S3, ESI†). These effects additionally explain the reasons for the higher stability of anions formed from molecules with the catechol moiety.

### Ionization potential

When one of the electrons is lost, the respective radical cation is formed. Generally, molecules with lower IP values are readily engaged in chemical reactions with free radicals.[58] All the investigated molecules have somewhat similar values for the IP (Table 1). This step requires almost 250 kJ mol$^{-1}$ less energy in polar solvents than in benzene. The IP values are the lowest

for L-DOPA in all solvents. The introduction of the second hydroxyl group does not influence this value, which is proven when dopamine and DOPAC are compared to 3-MT and homovanillic acid, respectively. This step in the SET-PT mechanism is energetically less probable than the first step of the SPLET or HAT/PCET mechanisms; therefore, it cannot be considered as dominant in solution.

### Antiradical mechanisms in water, methanol, and benzene

The antiradical activity of catecholamines and metabolites of dopamine was proven through the experiments with DPPH. The possible mechanisms can be discussed based on the thermodynamic parameters (BDE, IP, PDE, PA, and ETE) calculated in different solvents. The lowest value implies the preferability of the selected mechanism. The thermodynamic parameters prove that significant antiradical activity can be expected for all the investigated molecules. The presence of the second hydroxyl group attached to the aromatic ring lowers the value of the thermodynamic parameters, implying the importance of the catechol moiety. Because of the resonance effect in $-COO^-$, carboxyl groups have low PA values, which makes this structural parameter important for the radical scavenging activity. When both of the structural parameters are taken into consideration, L-DOPA and DOPAC have the highest probability of being good antiradical molecules, which was shown in the experimental section. A comparison of the first step in each of the three mechanisms (BDE, IP, and PA) shows that the values of the IP are the highest, which makes the SET-PT mechanism less probable compared to the other two in both solvents. In polar solvents, the PA values are lower than the BDE, while in benzene the opposite applies. In a non-polar environment, the difference between the BDE and the PA is much lower, which implies the competitiveness of both mechanisms. This difference in polar solvents is more than 200 kJ $mol^{-1}$, indicating the heterolytic dissociation of OH bonds and the SPLET mechanism as the prevailing one in polar environments. In order to prove this, a more detailed kinetic description is given for the HAT/PCET and SPLET mechanisms in the two following sections.

### HAT *versus* PCET mechanism

According to the EPR measurements that were previously carried out, the HAT mechanism is considered as the dominant one for the investigated compounds.[30,59] The hydrogen exchange reaction between four selected catecholamines and DPPH was studied using the M06-2X/6-31G(d,p) level of theory in vacuum. Corresponding transition state structures were obtained for dopamine, epinephrine, norepinephrine, and L-DOPA, as the most abundant and biochemically most important of the investigated molecules. The coordinates for transition state structures are given in Tables S4–S7 (ESI†).

From the thermodynamically most favourable position determined in the first part (*p*-OH group with respect to the aliphatic chain), only a single transition state is obtained for each of these molecules. However, it is expected that there are several other possible reaction pathways for hydrogen exchange through other investigated groups presented in the previous sections. This is especially true due to the possibility of hydrogen bond formation, which can be an important parameter for this mechanism as suggested in the literature.[60,61] All the investigated reactions are described additionally by application of a transition state theory that incorporates the quantum mechanical tunnelling effect. The transition state structure between dopamine and DPPH is given in Fig. 3.

The activation energies, rate constants, and the changes in the Gibbs free energy of the reactions are given in Table 3. The obtained reaction constants are similar for the investigated molecules, although slightly lower for dopamine. These values are in good agreement with research performed on similar molecules, namely phenol, 4-MeO-phenol, and 3-MeO-phenol, in the extensive investigation of Foti and coworkers,[62] which aimed to compare the theoretically and experimentally obtained values for energies of activation and rate constants. The experimental reaction constants for the reactions of dopamine, epinephrine, norepinephrine, and L-DOPA with the galvinoxyl radical[30] were of the same order of magnitude as for the reactions investigated here. It should be kept in mind that all the transition state structures were investigated in vacuum, while in the experimental measurements, a significant solvent effect was proven.[63]

One of the questions raised in this research was whether the reaction occurs through the HAT or the PCET mechanism. Both the mechanisms have important biological implications, as discussed in the introduction. Several techniques for distinguishing between these two mechanisms are used in the study. One of the common requirements for the PCET mechanism, the formation of a hydrogen bond[35,36] in the pre-reaction complex and transition state, is fulfilled here. If present, this requirement is usually insufficient as discussed by Mayer and co-workers.[36] From a structural point of view, the angle $\Theta$(O–H–N) is 165°, which deviates from linearity because of steric hindrance,[62] while in the "pure" HAT mechanism, this angle should be close to 180°. The dihedral angles can also be used to differentiate between the HAT and PCET mechanisms. If the transferring H atom is in plane with C–N–N and O–C–C, then the dominating mechanism is HAT (angle is 0°), while for PCET, this angle is 90°. The angles in the dopamine-DPPH complex have the following values: $\varphi$(H–O–C–C) = 45° and

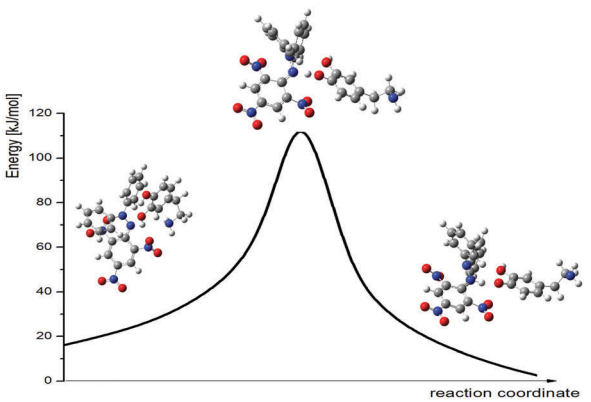


Fig. 3 The reaction pathway for the reaction of dopamine and DPPH.

 

Table 3 Values for the transition-state theory quantities

| Reaction | $\Delta G^{\ddagger}$ (kJ mol$^{-1}$) | $k^{TST}$ (s$^{-1}$) | $\Delta G_r$ (kJ mol$^{-1}$) |
|---|---|---|---|
| L-DOPA + DPPH$^{\bullet}$ | 67.6 | 8.8 | 15.3 |
| Dopamine + DPPH$^{\bullet}$ | 77.1 | $1.9 \times 10^{-1}$ | 19.3 |
| Norepinephrine + DPPH$^{\bullet}$ | 60.1 | $1.8 \times 10^{2}$ | 2.59 |
| Epinephrine + DPPH$^{\bullet}$ | 56.4 | $8.2 \times 10^{2}$ | −0.88 |

$\varphi$(H–N–N–C) = 43°. The structural features for the rest of the transition state complexes are within 1° of the respective values for the dopamine–DPPH reaction. This indicates that the transition state structure deviates from both mechanisms, which is probably due to steric effects.

One of the methods of distinguishing between the HAT and PCET mechanisms is by investigation of the SOMO density surface.[64] The HAT mechanism is characterized by a significant SOMO density along the donor-H-acceptor axis. On the other hand, PCET involves p-type orbitals that are orthogonal to the transition vector. The SOMO orbital of the dopamine-DPPH transition state is shown in Fig. 4, with the enlarged section showing the part of interest. As can be seen, the orbitals included in this transition state deviate from linearity, although there is significant SOMO density along the reaction axis, which gives partial characteristics of both mechanisms. The H-transferring atom interacts with the p-type orbitals of the N atom and the oxygen lone pair orbitals, as observed in similar molecules.[62]

A review paper by Galano[64] proposes a simple way to differentiate between the two mechanisms, which is based on the change in charge and spin density on the H-donor, H-acceptor, and transferring H atoms along the reaction coordinate. The sign of the charge on the donating and accepting atoms is modified along the coordinate for the PCET mechanism, while in HAT, charges stay negative for the whole reaction.[65] As well as the sign of the charge, the shape of the curve for the change in spin density and charge can be a distinguishing factor. A smooth change in the atomic charge indicates the HAT mechanism, while PCET is characterized by an abrupt jump in the value of this parameter around the position of the transition state structure. Data for the partial charges and spin density for the reaction complex, the transition state, and the product complex between dopamine and the DPPH radical are given in Table S4 (ESI†). The charges on oxygen and nitrogen are negative in all the investigated structures with no change in sign, while the charge on the hydrogen atom is ~0.5 *e*, which falls between the values obtained by Sirjoosingh and Hammes-Schiffer[65] for systems with pure PCET and HAT mechanisms. Fig. 5 and Fig. S9 (ESI†) present the change in atomic charge and spin density for relevant atoms in the reaction *versus* the reaction coordinate obtained from the IRC. The change in charge of the oxygen and nitrogen atoms along the coordinate is relatively smooth, but a significant difference is observed around the transition state although without intersection of the two curves. When the dependence of the spin density is compared to Fig. 8 from ref. 64. It can be deduced that the shape of the curve has the characteristics of both mechanisms. This analysis leads to the same conclusion as the structural and SOMO orbital investigations, that both mechanisms are present.

Because of the complexity of the radical structure and steric hindrance, the reaction between dopamine (and other catecholamines) cannot be described purely as HAT or PCET. The investigated system falls into the explanation given by Skone and co-workers, who suggested that the actual differentiation of these mechanisms is not possible in all cases because of the quantum mechanical behaviour of protons and electrons.[35,66]

## SPLET mechanism

The thermodynamic parameters governing the first step in SPLET are proven to be lower than for HAT/PCET (Table 2); therefore, this should not be the limiting step in the process of the antioxidant activity. The second step in SPLET is electron transfer from the antioxidant anion to the radical, and from Table 2, it can be concluded that this is energetically less favourable than HAT/PCET or the first step in SPLET. Kinetic parameters for this reaction were investigated using the Marcus

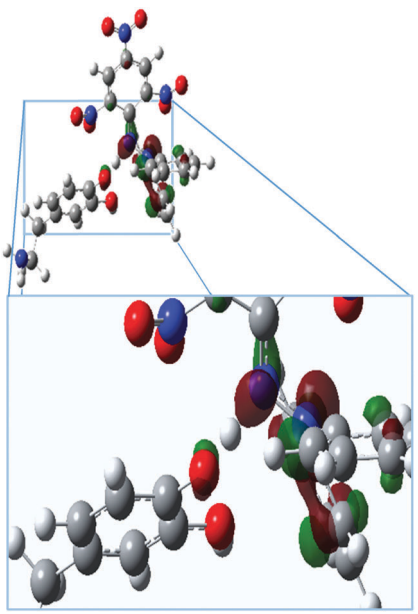

Fig. 4 SOMO orbital of the transition state between dopamine and DPPH.

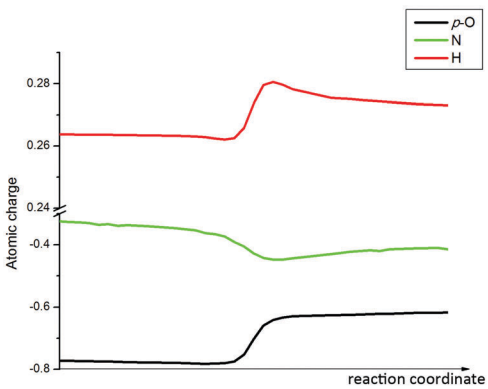


Fig. 5 Atomic charge change along the reaction coordinate for the relevant atoms for the reaction between dopamine and DPPH.

Table 4 Results related to electron transfer from L-DOPA, dopamine, epinephrine, and norepinephrine anions to DPPH• in the gas phase

| | $\Delta G^{\ddagger}_{ET}$ (kJ mol$^{-1}$) | $\Delta G^{0}_{ET}$ (kJ mol$^{-1}$) | $\lambda$ (kJ mol$^{-1}$) | $k_d$ (M$^{-1}$ s$^{-1}$) | $k_{TST}$ (M$^{-1}$ s$^{-1}$) | $k_{app}$ (M$^{-1}$ s$^{-1}$) |
|---|---|---|---|---|---|---|
| L-DOPA$^-$ + DPPH• | 2.7 | −64.5 | 43.0 | $3.33 \times 10^6$ | $2.11 \times 10^{12}$ | $3.33 \times 10^6$ |
| DopamineA$^-$ + DPPH• | 22.6 | −102.3 | 41.2 | $3.34 \times 10^6$ | $6.85 \times 10^8$ | $3.32 \times 10^6$ |
| EpinephrineA$^-$ + DPPH• | 25.6 | −106.3 | 41.3 | $3.34 \times 10^6$ | $2.02 \times 10^8$ | $3.29 \times 10^6$ |
| NorepinephrineA$^-$ + DPPH• | 31.0 | −107.5 | 38.4 | $3.33 \times 10^6$ | $2.27 \times 10^7$ | $2.91 \times 10^6$ |



theory as explained in the Computational section. Table 4 gives the activation free energy, the free energy of reaction for electron transfer, and the reorganisation energy, as well as the rate constant from TST, the rate constant for the irreversible bimolecular diffusion-controlled reaction, and the apparent rate constant.

The given results lead to the conclusion that the rates of the ET reaction are of the order of $10^6$ M$^{-1}$ s$^{-1}$ for all the investigated molecules. The obtained rate constants from the transition state theory are much larger, but because of the diffusion, the apparent rate constant is of the above-mentioned order. All the reactions are exergonic. The actual values for different catecholamines are comparable, leading to the conclusion that there are no significant but small differences, with L-DOPA having the largest value. This is well reflected in the experimental results. It is important to compare the rates of HAT/PCET and the ETE from Tables 3 and 4. The activation free energy is much lower in case of the ET, rate constants are larger ($10^6$ compared to $10^1$ M$^{-1}$ s$^{-1}$), and the free energy of reaction is negative. All this proves that ET is faster than HAT/PCET. This result, together with the lower change in enthalpy for the first step of SPLET, when compared to HAT/PCET, leads to the conclusion that SPLET is the dominant mechanism for the reaction between L-DOPA, dopamine, epinephrine, and norepinephrine with the DPPH radical in methanol. Because of the resemblance of these molecules to the rest of the investigated molecules, this conclusion can be generalized to all the catecholamines in this study.

## Conclusions

In this contribution, the antiradical potency of naturally occurring catecholamines (catechol, dopamine, epinephrine, norepinephrine, and L-DOPA) and three metabolites of dopamine (homovanillic acid, DOPAC, and 3-MT) has been investigated. Experimentally, the antiradical activity has been proven in the reaction with the DPPH radical in methanol. All the investigated molecules, except for 3-MT and homovanillic acid, have antiradical activity comparable to the most potent antiradical molecules. The theoretical consideration through the calculation of the thermodynamic parameters, for the most common antiradical mechanisms, has shown that all the present species can be considered as good antiradicals, except homovanillic acid and 3-MT, which have only one OH group attached to the aromatic ring. This has been explained by the stabilization effect of the intramolecular hydrogen bond present in radicals and anions of the corresponding molecules. The lowest values for the thermodynamic parameters have been calculated for the *p*-hydroxyl group. The additional groups, carboxyl, amino, and hydroxyl groups attached to the aliphatic chain, can also be sites of hydrogen exchange. The obtained results pointed to SET-PT as an implausible radical scavenging mechanism due to high IP values. The SPLET mechanism is the most probable in polar solvents, while in non-polar solvents SPLET and HAT/PCET are competitive.

The transition state structures for the reactions of dopamine, epinephrine, norepinephrine, and L-DOPA with the DPPH radical were used for the differentiation of the HAT and PCET mechanisms through several suggested strategies. The conclusion based on the geometry, SOMO orbital density, and changes in charge and spin density of the atoms of interest, is that both mechanisms are present because of the steric hindrance of the radical, which influences its stability towards the antiradical molecules. The rate constants for the HAT/PCET reaction are of the order of $10^{-1}$ to $10^2$ M$^{-1}$ s$^{-1}$. The second step of SPLET was also kinetically investigated by application of the Marcus theory. The values for the rate constants, after corrections due to diffusion, were of the order of $10^6$ M$^{-1}$ s$^{-1}$. This finding, together with the higher thermodynamic preferability of the first step of SPLET compared to HAT/PCET, proved that the dominant mechanism of the antiradical activity of catecholamines in polar solvents is SPLET.

## Acknowledgements

The authors would like to thank the Ministry of Education, Science and Technological Development of the Republic of Serbia for the support through Grants No. 172015 and 172040.

## Notes and references

1 I. Fridovich, *Science*, 1978, **201**, 875–880.
2 H. Sies, *Oxidative Stress: Oxidants and Antioxidants*, Academic Press, New York, 1991.
3 B. Halliwell and J. M. C. Gutteridge, *Free Radicals in Biology and Medicine*, Clarendon Press, Oxford, 3rd edn, 1999.
4 P. Jenner, *Ann. Neurol.*, 2003, **53**, S26–S38.
5 L. Lyras, N. J. Cairns, A. Jenner, P. Jenner and B. Halliwell, *J. Neurochem.*, 1997, **68**, 2061–2069.
6 L. M. Sayre, M. a Smith and G. Perry, *Curr. Med. Chem.*, 2001, **8**, 721–738.
7 P. K. Toshniwal and E. J. Zarling, *Neurochem. Res.*, 1992, **17**, 205–207.
8 J. A. Klein and S. L. Ackerman, *J. Clin. Invest.*, 2003, **111**, 785–793.
9 J. Zhang, G. Perry, M. A. Smith, D. Robertson, S. J. Olson, D. G. Graham and T. J. Montine, *Am. J. Pathol.*, 1999, **154**, 1423–1429.

 

10 O. Hornykiewicz, *Mov. Disord.*, 2002, **17**, 501–508.
11 R. M. Berman, M. Narasimhan, H. L. Miller, A. Anand, A. Cappiello, D. A. Oren, G. R. Heninger and D. S. Charney, *Arch. Gen. Psychiatry*, 1999, **56**, 395–403.
12 H. M. Kravitz, H. C. Sabelli and J. Fawcett, *J. Am. Osteopath. Assoc.*, 1984, **84**, 119–123.
13 L. Pauling, *Science*, 1968, **160**, 265–271.
14 T. Shimizu, Y. Nakanishi, M. Nakahara, N. Wada, Y. Moro-Oka, T. Hirano, T. Konishi and S. Matsugo, *J. Clin. Biochem. Nutr.*, 2010, **47**, 181–190.
15 A. J. Lopes Jesus, S. Jarmelo, R. Fausto and I. Reva, *Spectrochim. Acta, Part A*, 2015, **140**, 54–64.
16 J. Laranjinha and E. Cadenas, *J. Neurochem.*, 2002, **81**, 892–900.
17 M. Samsonowicz, M. Kowczyk-Sadowy, E. Regulska and W. Lewandowski, *Spectrochim. Acta, Part A*, 2014, **118**, 1068–1074.
18 T. D. Sotnikova, J.-M. Beaulieu, S. Espinoza, B. Masri, X. Zhang, A. Salahpour, L. S. Barak, M. G. Caron and R. R. Gainetdinov, *PLoS One*, 2010, **5**, e13452.
19 J. W. M. Lenders, K. Pacak, M. M. Walther, W. M. Linehan, M. Mannelli, P. Friberg, H. R. Keiser, D. S. Goldstein and G. Eisenhofer, *JAMA*, 2002, **287**, 356–368.
20 S. W. Kim, H. S. Ko, V. L. Dawson and T. M. Dawson, *Drug Discovery Today: Dis. Mech.*, 2005, **2**, 427–433.
21 J. C. Fitzgerald and H. Plun-Favreau, *FEBS J.*, 2008, **275**, 5758–5766.
22 K. Jodko-Piórecka and G. Litwinienko, *Free Radicals Biol. Med.*, 2015, **83**, 1–11.
23 T. L. Lemke, D. A. Williams, W. O. Foye and S. W. Zito, *Foye's principles of medicinal chemistry*, Wolters Kluwer Health/Lippincott Williams & Wilkins, 2013.
24 J. Smythies, *Antioxid. Redox Signaling*, 2000, **2**, 575–583.
25 Y. Gilgun-Sherki, E. Melamed and D. Offen, *Neuropharmacology*, 2001, **40**, 959–975.
26 C. Sârbu and D. Casoni, *Open Chem.*, 2013, **11**, 679–688.
27 A. Kladna, P. Berczynski, I. Kruk, T. Michalska and A.-E. HY, *Luminescence*, 2013, **28**, 450–455.
28 A. Kładna, P. Berczyński, I. Kruk, T. Michalska and H. Y. Aboul-Enein, *Luminescence*, 2012, **27**, 473–477.
29 İ. Gülçin, *Chem.-Biol. Interact.*, 2009, **179**, 71–80.
30 T. Kawashima, K. Ohkubo and S. Fukuzumi, *J. Phys. Chem. B*, 2010, **114**, 675–680.
31 C. Iuga, J. R. Alvarez-Idaboy and A. Vivier-Bunge, *J. Phys. Chem. B*, 2011, **115**, 12234–12246.
32 R. Álvarez-Diduk and A. Galano, *J. Phys. Chem. B*, 2015, **119**, 3479–3491.
33 E. Klein, V. Lukeš and M. Ilčin, *Chem. Phys.*, 2007, **336**, 51–57.
34 G. Litwinienko and K. U. Ingold, *Acc. Chem. Res.*, 2007, **40**, 222–230.
35 G. DiLabio and E. Johnson, *J. Am. Chem. Soc.*, 2007, **129**, 6199–6203.
36 J. M. Mayer, D. A. Hrovat, J. L. Thomas and W. T. Borden, *J. Am. Chem. Soc.*, 2002, **124**, 11142–11147.
37 N. Nenadis and M. Tsimidou, *J. Am. Oil Chem. Soc.*, 2002, **79**, 1191–1195.
38 M. J. Frisch, G. W. Trucks, H. B. Schlegel, G. E. Scuseria, M. A. Robb, J. R. Cheeseman, G. Scalmani, V. Barone, B. Mennucci, G. A. Petersson, H. Nakatsuji, M. Caricato, X. Li, H. P. Hratchian, A. F. Izmaylov, J. Bloino, G. Zheng, J. L. Sonnenberg, M. Hada, M. Ehara, K. Toyota, R. Fukuda, J. Hasegawa, M. Ishida, T. Nakajima, Y. Honda, O. Kitao, H. Nakai, T. Vreven, J. A. Montgomery, Jr., J. E. Peralta, F. Ogliaro, M. Bearpark, J. J. Heyd, E. Brothers, K. N. Kudin, V. N. Staroverov, R. Kobayashi, J. Normand, K. Raghavachari, A. Rendell, J. C. Burant, S. S. Iyengar, J. Tomasi, M. Cossi, N. Rega, J. M. Millam, M. Klene, J. E. Knox, J. B. Cross, V. Bakken, C. Adamo, J. Jaramillo, R. Gomperts, R. E. Stratmann, O. Yazyev, A. J. Austin, R. Cammi, C. Pomelli, J. W. Ochterski, R. L. Martin, K. Morokuma, V. G. Zakrzewski, G. A. Voth, P. Salvador, J. J. Dannenberg, S. Dapprich, A. D. Daniels, O. Farkas, J. B. Foresman, J. V. Ortiz, J. Cioslowski and D. J. Fox, *Gaussian 09, Revision C.01*, Gaussian, Inc., Wallingford CT, 2009.
39 Y. Zhao and D. G. Truhlar, *Theor. Chem. Acc.*, 2007, **120**, 215–241.
40 T. H. Dunning, *J. Chem. Phys.*, 1989, **90**, 1007.
41 A. Garzón, I. Bravo, A. J. Barbero and J. Albaladejo, *J. Agric. Food Chem.*, 2014, **62**, 9705–9710.
42 A. Amić, Z. Marković, J. M. D. Marković, S. Jeremić, B. Lučić and D. Amić, *Comput. Biol. Chem.*, 2016, **65**, 45–53.
43 M. M. Kabanda, V. T. Tran, K. M. Seema, K. R. N. Serobatse, T. J. Tsiepe, Q. T. Tran and E. E. Ebenso, *Mol. Phys.*, 2015, **113**, 683–697.
44 A. V. Marenich, C. J. Cramer and D. G. Truhlar, *J. Phys. Chem. B*, 2009, **113**, 6378–6396.
45 J. P. Foster and F. Weinhold, *J. Am. Chem. Soc.*, 1980, **102**, 7211–7218.
46 M. Filipović, Z. Marković, J. Đorović, J. D. Marković, B. Lučić and D. Amić, *C. R. Chim.*, 2015, **18**, 492–498.
47 Z. Marković, J. Đorović, Z. D. Petrović, V. P. Petrović and D. Simijonović, *J. Mol. Model.*, 2015, **21**, 293.
48 Z. Marković, J. Tošović, D. Milenković and S. Marković, *Comput. Theor. Chem.*, 2016, **1077**, 11–17.
49 W. T. Duncan, R. L. Bell and T. N. Truong, *J. Comput. Chem.*, 1998, **19**, 1039–1052.
50 R. A. Marcus, *Angew. Chem., Int. Ed.*, 1993, **32**, 1111–1121.
51 F. C. Collins and G. E. Kimball, *J. Colloid Sci.*, 1949, **4**, 425–437.
52 M. C. Foti, *J. Agric. Food Chem.*, 2015, **63**, 8765–8776.
53 A. Lagutschenkov, J. Langer, G. Berden, J. Oomens and O. Dopfer, *Phys. Chem. Chem. Phys.*, 2011, **13**, 2815–2823.
54 L. C. Snoek, T. Van Mourik and J. P. Simons, *Mol. Phys.*, 2003, **101**, 1239–1248.
55 T. van Mourik, *Phys. Chem. Chem. Phys.*, 2004, **6**, 2827–2837.
56 B. Edwin and I. Hubert Joe, *J. Mol. Struct.*, 2013, **1034**, 119–127.
57 L. M. LeBlanc, A. F. Paré, J. Jean-Francois, M. J. G. Hébert, M. E. Surette and M. Touaibia, *Molecules*, 2012, **17**, 14637–14650.
58 Z. D. Petrović, J. Đorović, D. Simijonović, V. P. Petrović and Z. Marković, *RSC Adv.*, 2015, **5**, 24094–24100.
59 K. Ohkubo, Y. Moro-oka and S. Fukuzumi, *Org. Biomol. Chem.*, 2006, **4**, 999.

60 M. C. Foti, R. Amorati, G. F. Pedulli, C. Daquino, D. A. Pratt and K. U. Ingold, *J. Org. Chem.*, 2010, **75**, 4434–4440.
61 M. C. Foti, E. R. Johnson, M. R. Vinqvist, J. S. Wright, L. R. C. Barclay and K. U. Ingold, *J. Org. Chem.*, 2002, **67**, 5190–5196.
62 M. C. Foti, C. Daquino, I. D. Mackie, G. A. DiLabio and K. U. Ingold, *J. Org. Chem.*, 2008, **73**, 9270–9282.
63 M. Foti and G. Ruberto, *J. Agric. Food Chem.*, 2001, **49**, 342–348.
64 A. Galano, *J. Mex. Chem. Soc.*, 2015, **59**, 231–262.
65 A. Sirjoosingh and S. Hammes-Schiffer, *J. Phys. Chem. A*, 2011, **115**, 2367–2377.
66 J. H. Skone, A. V. Soudackov and S. Hammes-Schiffer, *J. Am. Chem. Soc.*, 2006, **128**, 16655–16663.